

Supplemental Methods, Figures and References

Supplementary Materials and Methods

Antimicrobial Treatment

Mice (5 *Tff1*-WT and 5 *Tff1*-KO) were housed in individually ventilated cages supplied with autoclaved filtered water and rodent chow. Antibiotic treatment started at 3 weeks of age, immediately after weaning. Mice were given autoclaved drinking water containing 0.68 mg/mL metronidazole and 0.34 mg/mL ciprofloxacin until the age of 12 weeks (1). Upon completion of the treatment, mice received autoclaved water and rodent chow and were handled in sterile conditions for 12 weeks. The mice were sacrificed and stomach tissues were collected for histological evaluation.

Treatment with Celecoxib

At the age of three weeks, immediately after weaning, twenty *Tff1*-knockout mice were divided into two equal groups of ten each; one control and one experimental group. The control group received intra peritoneal injection of vehicle (5 μ l/g body weight). The vehicle consisted of propylene glycerol, polysorbate 80, benzyl alcohol, ethanol and water (40:0.5:1:10:48.5) (2). The experimental group received Celecoxib (10 μ g/g). Injections were given three times a week for two months. Animals were sacrificed and stomach tissues were collected for histological evaluation.

Rescue of Tff1 effects/signaling in Primary Gastric Epithelial Cells

Because TFF1 is a secreted protein, we decided to confirm the role of TFF1 in regulating NF- κ B ex-vivo in primary gastric epithelial cell cultures. We performed a rescue experiment using conditioned media from AGS-pcDNA and AGS-TFF1 cells. Primary gastric epithelial cells from pyloric antral region of *Tff1*-knockout mice were cultured in three parallel 8-well chambers for 24 hours. On the next day, cells were washed with PBS and media was replaced with either conditioned media from AGS-pcDNA (chamber A) or AGS-TFF1 cell lines culture (chambers B and C). After another 48 hours, cells in chambers A and B were processed for dual immunofluorescence staining with rabbit anti-NF- κ B p65 antibody (Gene Script)

and mouse anti-Zo1 antibody (ZYMED Laboratories, Invitrogen). Cells treated with AGS-TFF1 conditioned media in chamber C were washed with PBS and treated with AGS-pcDNA conditioned media. Following an additional 24 hours, these cells were processed for dual immunofluorescence staining as above. All experiments were performed in triplicates.

Supplemental Figure Legends

Figure S1.

A: Representative images of stomachs from *Tff1*-KO mice at 8 months of age and older showing large tumors in the antrum region. **B:** Ki-67 immunostaining (brown nuclei) in WT mice reveals dividing cells in the proliferative zone of the mucosa (left panel); in *Tff1*-KO, stained cells extended to the surface (right panel); original magnification, x10. **C&D:** Box plots representing the comparison of chronic and acute inflammation scores between *Tff1*-WT and *Tff1*-KO mice. **E&F:** Box plots representing the comparison of chronic and acute inflammation scores between male and female *Tff1*-KO mice, respectively. **G:** Comparison of Acute inflammation scores between different dysplastic lesions. **H:** Comparison of chronic inflammation scores between *Tff1*-WT and *Tff1*-KO treated with Ciprofloxacin and Metronidazole. Box-and-whisker plots were used depict the smallest value, lower quartile, mean, upper quartile, and largest value.

Figure S2. Morphological histology of different tissues from the same *Tff1*-KO mice

A-F: Hematoxylin & eosin (H&E) staining of representative histological features of gastrointestinal track (Stomach, Esophagus, and Colon) and other organs (Liver, Spleen and Thymus) from the same *Tff1*-knockout mouse. **A:** antro-pyloric area showing dysplasia (square) and infiltration of inflammatory cells (circle); original magnification x4. The inset in panel A displays a higher magnification (x40) of dysplastic glands. **B-F:** All other tissues appear to be normal; original magnification, x10 (B, D, E & F) and x20 (C).

Figure S3.

A-I: Validation of selected inflammatory genes from microarray results. Relative mRNA expression levels were examined in the antral gastric tissues from wild-type and *Tff1*-knockout mice at different ages. Horizontal bars indicate the mean and $p \leq 0.05$ was considered statistically significant.

Figure S4. Celecoxib treatment affects the development of gastric lesions in the *Tff1*-KO mice

A: Bars representing the comparison of frequency of dysplasia between vehicle (n=10) and celecoxib (n=10) treated *Tff1*-KO mice. **B&C:** qRT-PCR showing a decrease in mRNA expression of pro-inflammatory genes (*Cxcl1* and *Cxcl5*) in celecoxib-treated group normalized to Vehicle.

Figure S5: Inverse correlation between TFF1 and pIKK α/β expression

A: qRT-PCR representing the human *TFF1* gene expression in AGS TFF1 clone 1 & 2 normalized to AGS-pcDNA. **B:** Western Blot analysis showing the expression of pIKK α/β and total IKK β in AGS-pcDNA and AGS-TFF1 clone 1.

Figure S6: Expression of *Tff1* in mouse tissues

qRT-PCR of *Tff1* in tissues from *Tff1*-wild-type mice showing high expression levels in the pyloro-antral regions of the stomach. In contrast, *Tff1* expression was almost undetectable in different immune system organs: Thymus, Bone marrow (BM) and spleen.

Figure S7: Expression of TNFR1 and TNFR2.

A: qRT-PCR demonstrated high levels of *TNFR1* in AGS-pcDNA and AGS-TFF1 clones 1 and 2 whereas *TNFR2* levels were almost undetectable in the same cells. **B:** qRT-PCR showing similar levels of mRNA expression of *Tnfr1* in the stomach of *Tff1*-knockout and *Tff1*-wild type mice.

Figure S8: Downregulation of TFF1 mRNA in human gastric cancers

A: qRT-PCR analysis of 70 human gastric adenocarcinomas and 36 normal gastric epithelial tissues demonstrated a significant reduction in *TFF1* mRNA expression in tumor samples ($p<0.001$). **B:** qRT-PCR analysis of 15 matched gastric cancer (tumor) and adjacent non-tumor (normal) samples indicated that the *TFF1* expression was significantly downregulated in the tumor samples as compared to their adjacent histologically normal tissues ($P<0.01$).

SUPPLEMNTAL REFERNECES

1. Judd, L.M., Bredin, K., Kalantzis, A., Jenkins, B.J., Ernst, M., and Giraud, A.S. 2006. STAT3 activation regulates growth, inflammation, and vascularization in a mouse model of gastric tumorigenesis. *Gastroenterology* 131:1073-1085.
2. Zheng, X., Cui, X.X., Avila, G.E., Huang, M.T., Liu, Y., Patel, J., Kong, A.N., Paulino, R., Shih, W.J., Lin, Y., et al. 2007. Atorvastatin and celecoxib inhibit prostate PC-3 tumors in immunodeficient mice. *Clin Cancer Res* 13:5480-5487.

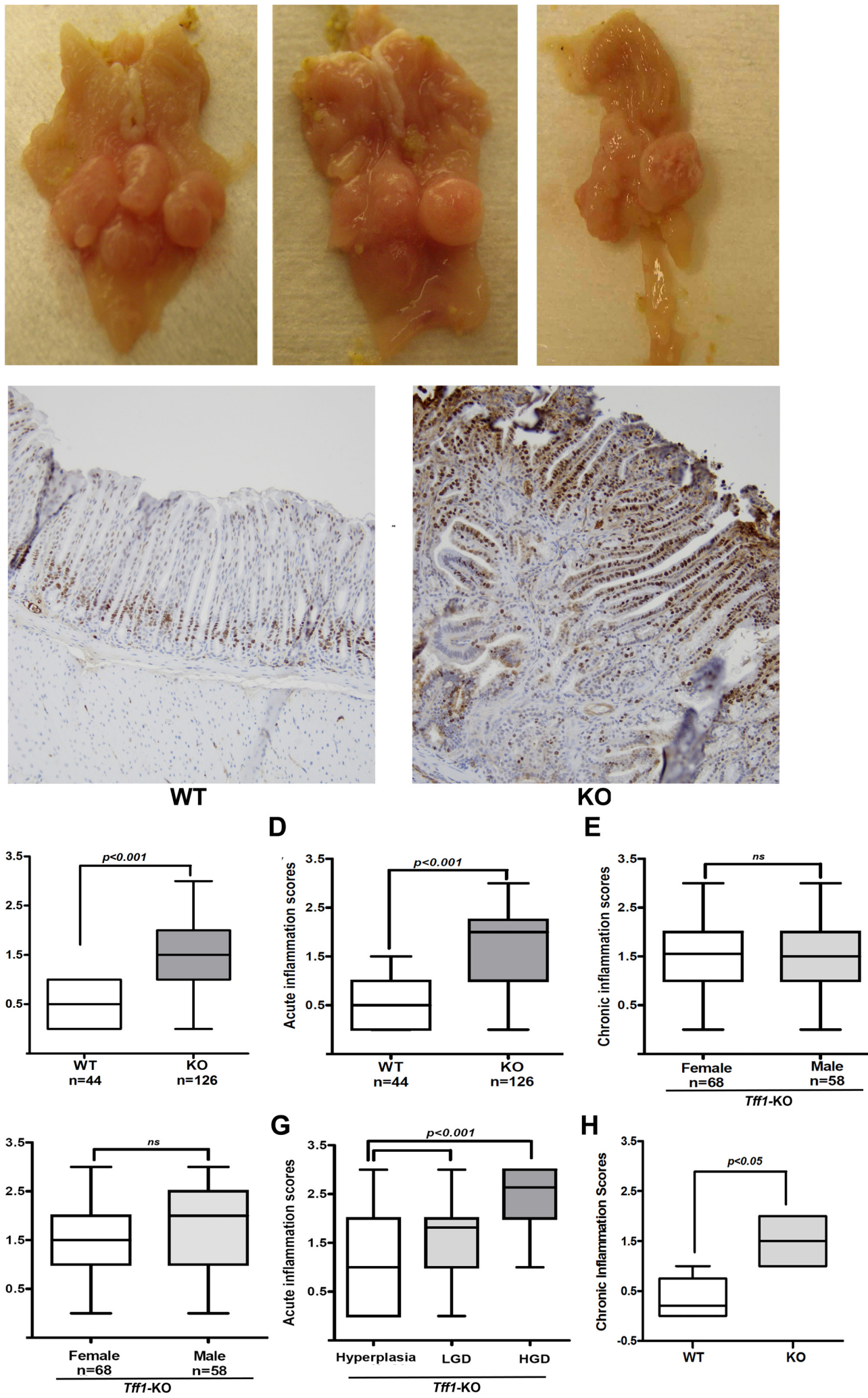


Figure S1. Soutto et al.

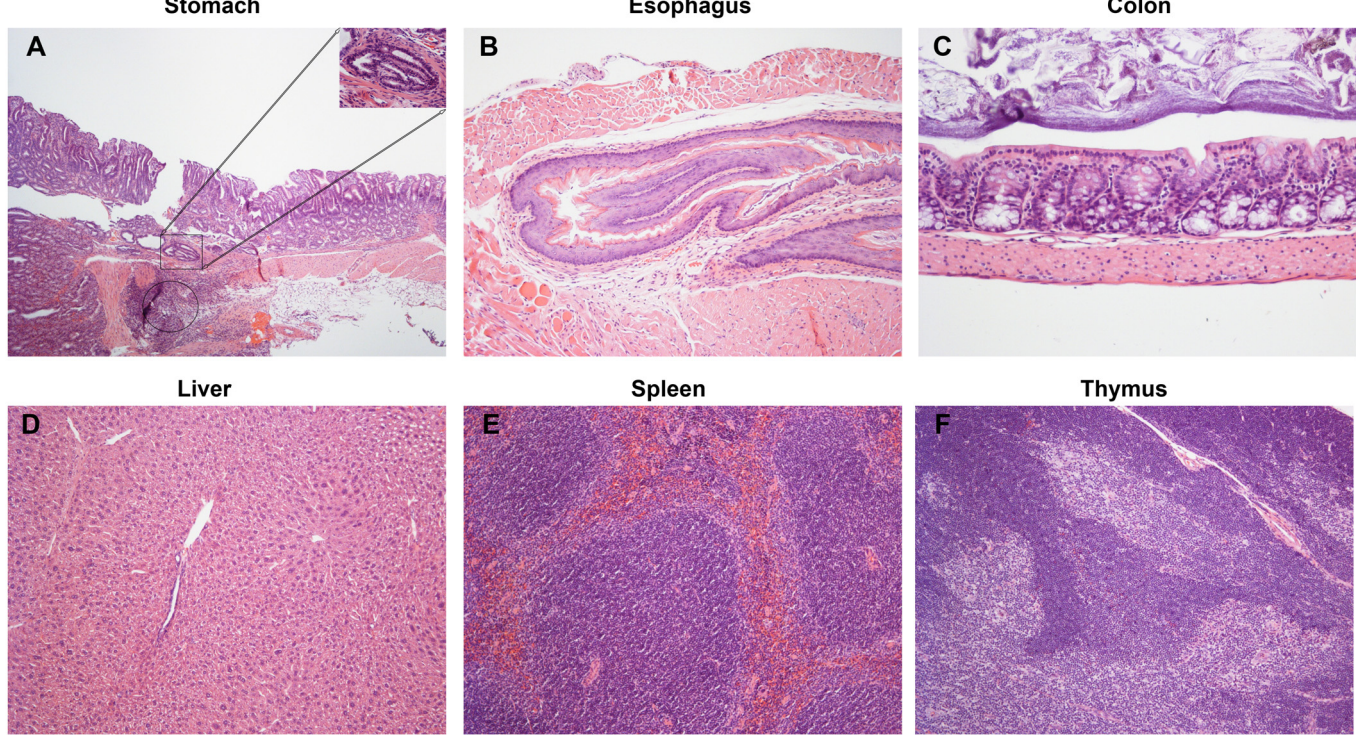


Figure S2. Soutto et al.

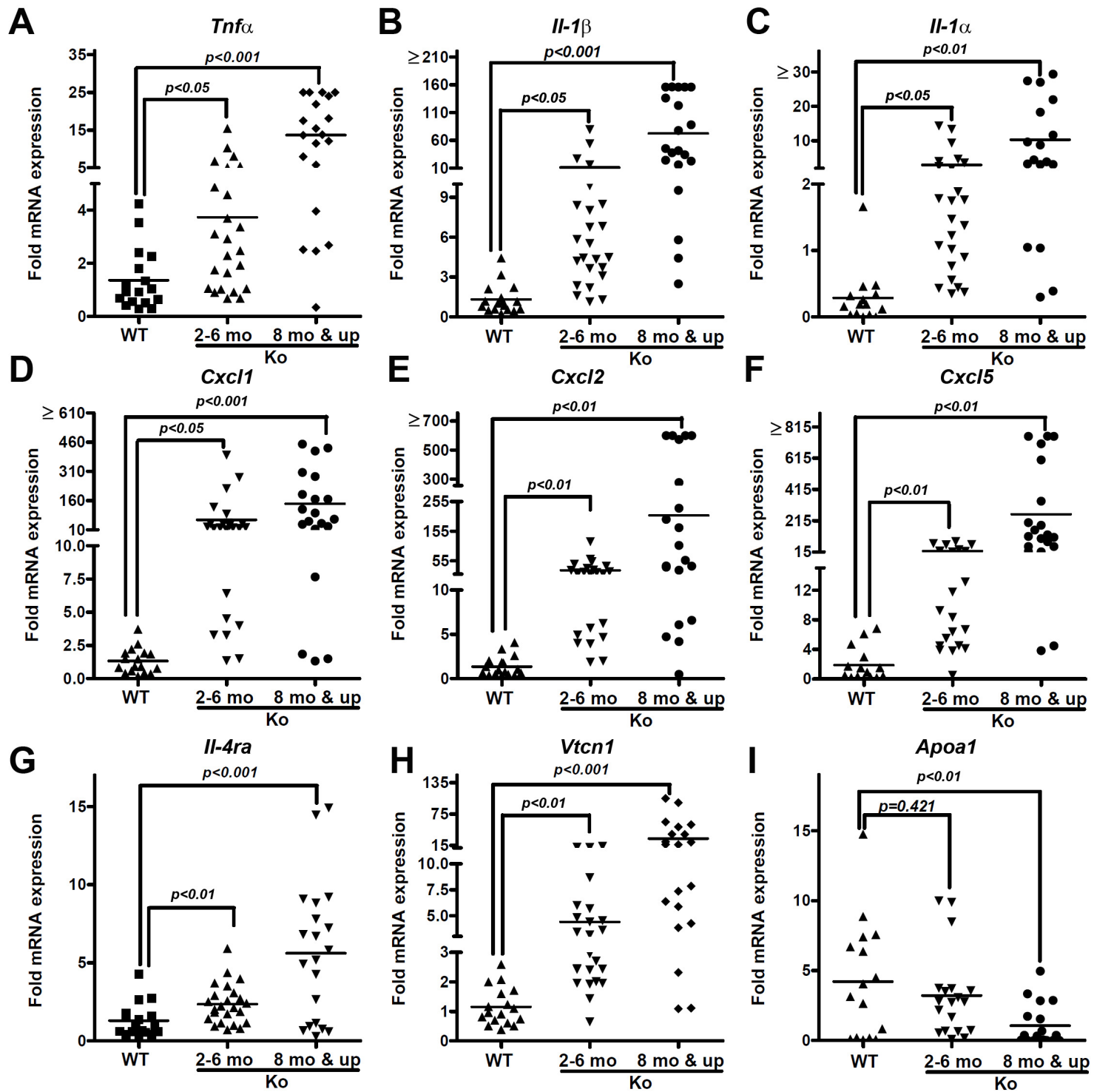


Figure S3. Soutto et al.

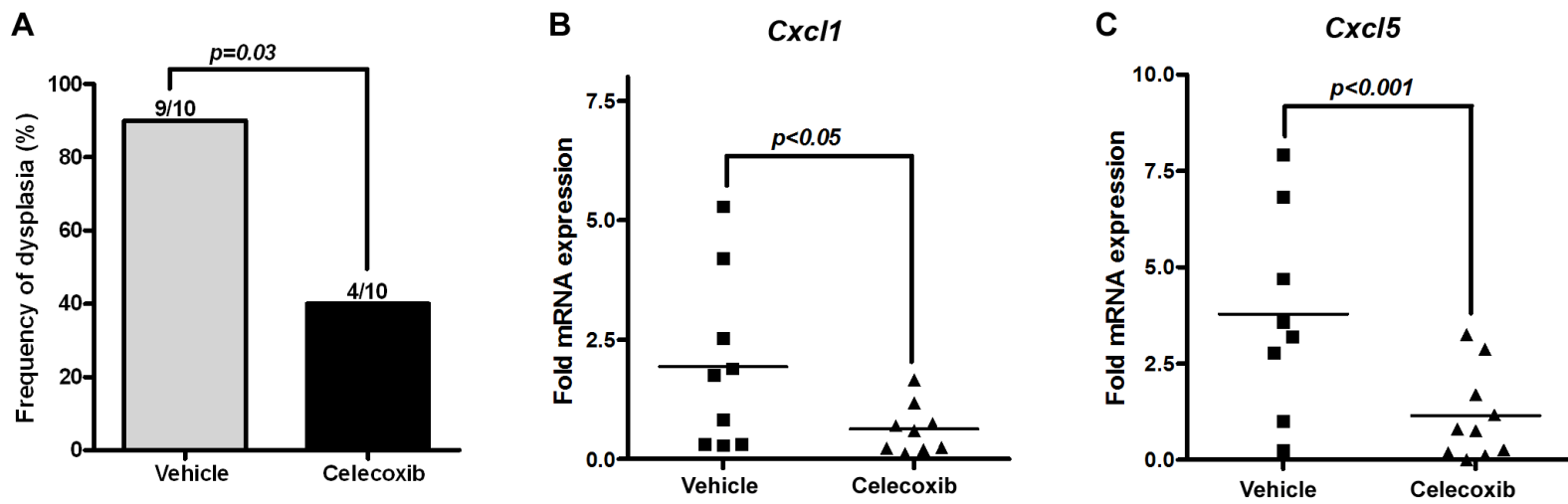


Figure S4, Soutto et al.

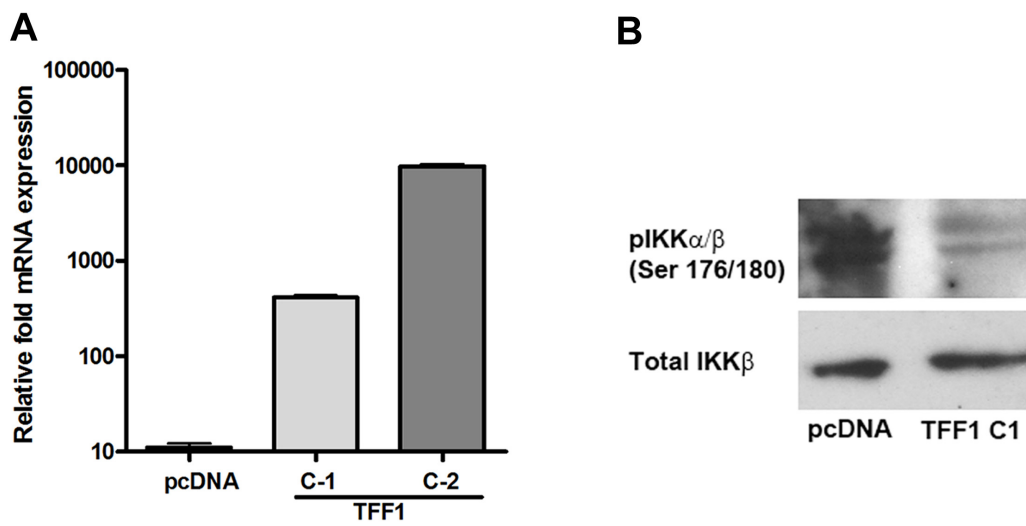


Figure S5. Soutto et al.

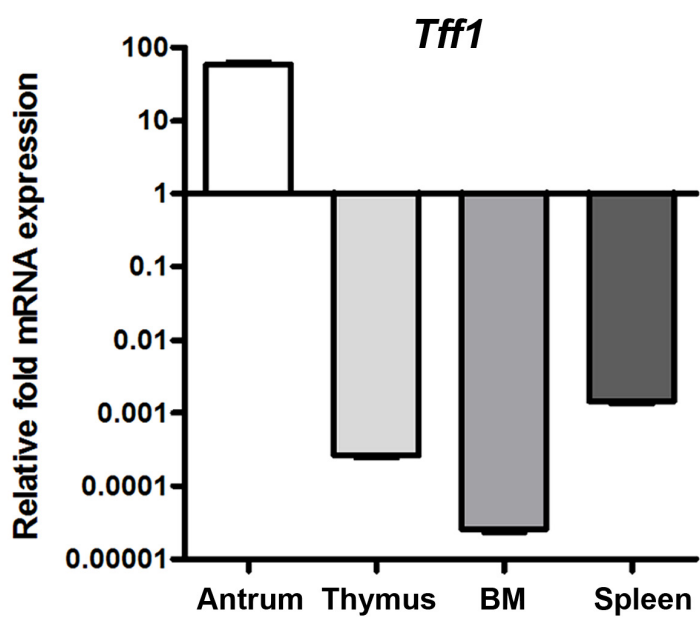


Figure S6. Soutto et al.

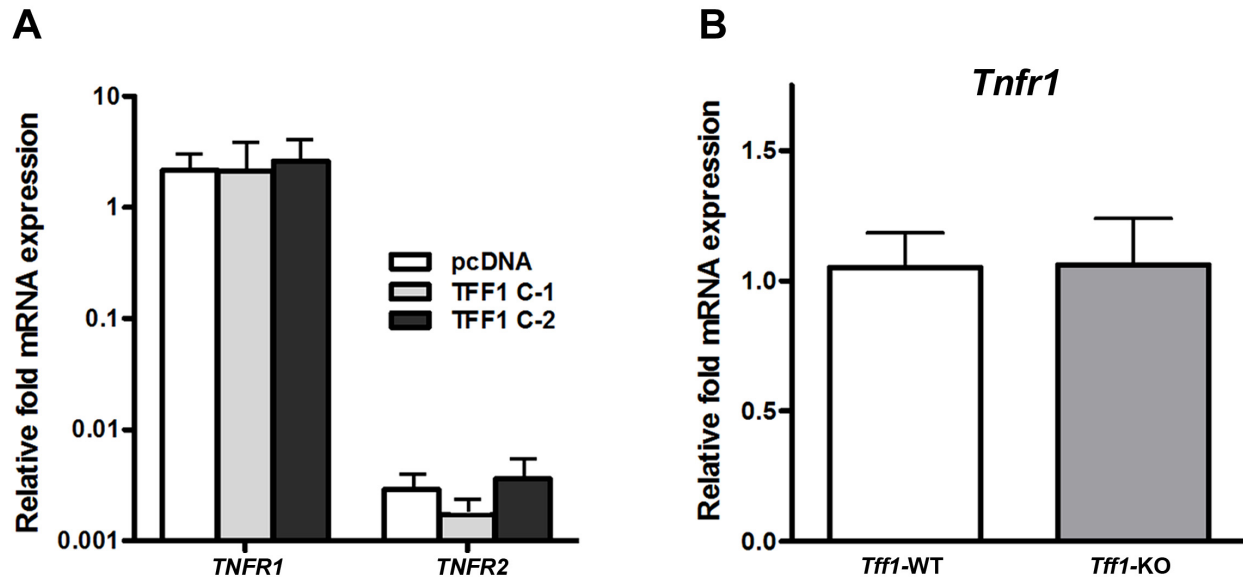


Figure S7. Soutto et al.

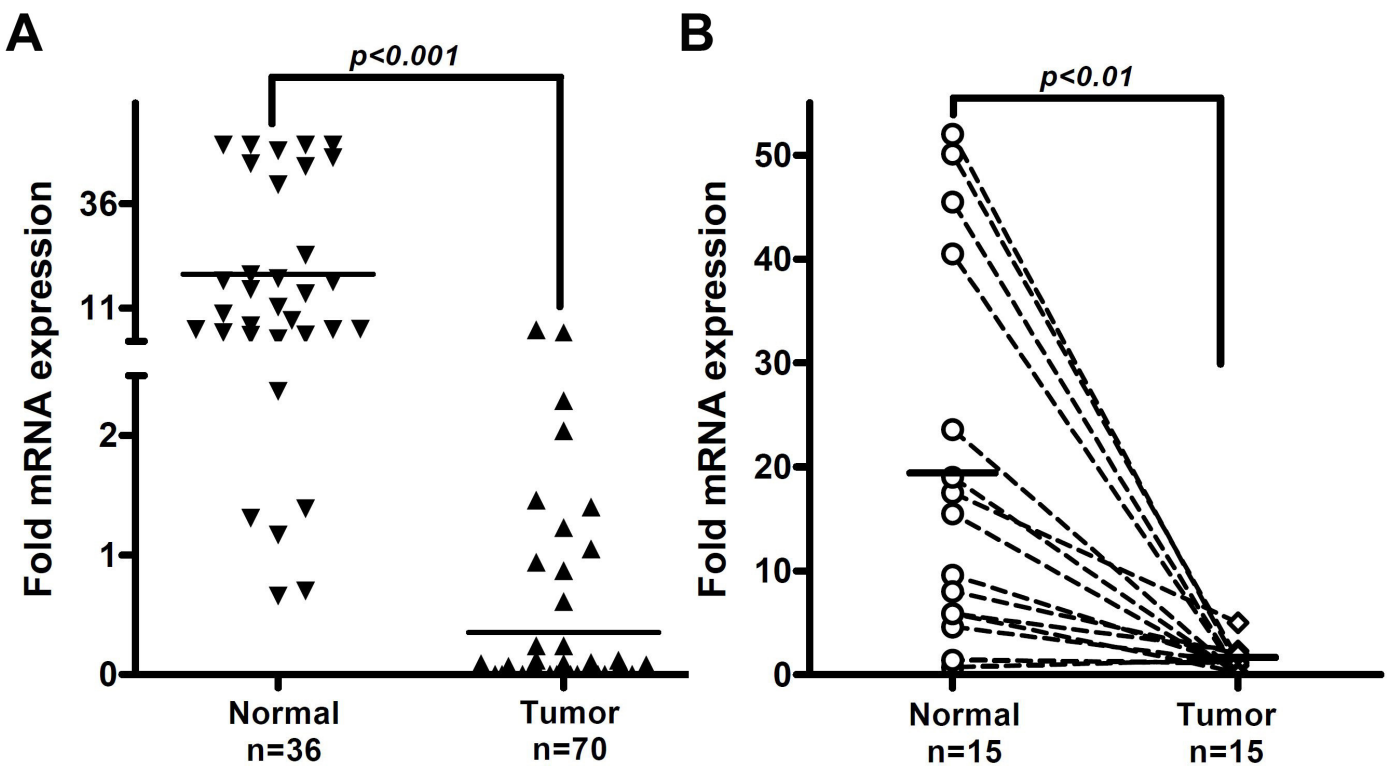


Figure S8. Soutto et al.

Supplemental Table 1. Fold change of inflammation-related genes in Tff1 KO vs WT

ID	Symbol	UGCluster	Fold (KO vs WT)		Chromosome	
			PValue	Cytoband	Name	
1450105_at	Adam10	Mm.3037	3.3	2.E-03	9 D	a disintegrin and metallopeptidase domain 10
1426619_at	Aim2	Mm.131453	3.3	2.E-03	1 H3	absent in melanoma 2
1419091_a_at	Anxa2	Mm.238343	2.9	7.E-04	9 C	annexin A2
1438840_x_at	Apoa1	Mm.26743	0.0	5.E-08	9 A2-A4	apolipoprotein A-I
1417761_at	Apoa4	Mm.4533	0.1	4.E-07	9 A5.2	apolipoprotein A-IV
1417776_at	Azgp1	Mm.30061	0.2	3.E-03	5 G2	alpha-2-glycoprotein 1, zinc
1422084_at	Bmx	Mm.504	3.0	2.E-02	X F	BMX non-receptor tyrosine kinase
1418021_at	C4b	Mm.439678	4.4	6.E-03	17 B1	complement component 4B (Child blood group)
1426165_a_at	Casp3	Mm.34405	3.1	4.E-03	8 B1.1	caspase 3
1417268_at	Cd14	Mm.3460	5.6	3.E-04	18 B2	CD14 antigen
1450884_at	Cd36	Mm.18628	0.0	5.E-06	5 A3	CD36 antigen
1423760_at	Cd44	Mm.423621	8.5	6.E-04	2 E2	CD44 antigen
1441907_s_at	Cd93	Mm.681	5.8	4.E-05	2 G3	CD93 antigen
1452532_x_at	Ceacam1	Mm.322502	6.2	4.E-04	7 A3	carcinoembryonic antigen-related cell adhesion molecule 1
1427767_a_at	Cftr	Mm.15621	7.6	1.E-02	6 3.1 cM	cystic fibrosis transmembrane conductance regulator homolog
1424495_a_at	Ckif	Mm.269219	3.2	8.E-05	8 D3	chemokine-like factor
1416953_at	Ctgf	Mm.390287	4.0	1.E-03	10 A3-B1	connective tissue growth factor
1457644_s_at	Cxcl1	Mm.21013	18.0	9.E-03	5 E-F	chemokine (C-X-C motif) ligand 1
1449984_at	Cxcl2	Mm.4979	14.4	1.E-02	5 E1	chemokine (C-X-C motif) ligand 2
1438148_at	Cxcl3	Mm.244289	8.6	3.E-02	5 E1	chemokine (C-X-C motif) ligand 3
1419728_at	Cxcl5	Mm.4660	6.3	8.E-03	5 E1	chemokine (C-X-C motif) ligand 5
1454268_a_at	Cyba	Mm.271671	3.1	3.E-04		cytochrome b-245, alpha polypeptide
1418287_a_at	Dmbt1	Mm.4138	5.1	2.E-04	7 F4	deleted in malignant brain tumors 1
1429021_at	Epha4	Mm.400747	4.1	2.E-04	1 C1-C5	Eph receptor A4
1417408_at	F3	Mm.273188	4.3	1.E-02	3 G1	coagulation factor III
1449269_at	F5	Mm.12900	5.8	7.E-03	1 H2.2	coagulation factor V
1423100_at	Fos	Mm.246513	3.4	3.E-04	12 D2	FBJ osteosarcoma oncogene
1422555_s_at	Gna13	Mm.193925	3.0	6.E-03	11 E1	guanine nucleotide binding protein, alpha 13
1425357_a_at	Grem1	Mm.166318	4.4	2.E-02	2 E4	gremlin 1
1418350_at	Hbegf	Mm.289681	3.9	1.E-03	18 B2	heparin-binding EGF-like growth factor
1427127_x_at	Hspa1b	Mm.372314	3.0	3.E-02	17 B1	heat shock protein 1B

1419647_a_at	Ier3	Mm.25613	3.6	6.E-04	17 B1	immediate early response 3
1449982_at	Il11	Mm.35814	3.8	3.E-02	7 A1	interleukin 11
1451775_s_at	Il13ra1	Mm.24208	5.4	5.E-04	X A3.3	interleukin 13 receptor, alpha 1
1421628_at	Il18r1	Mm.253664	3.4	2.E-03	1 B	interleukin 18 receptor 1
1421291_at	Il18rap	Mm.20466	3.5	1.E-02	1 B	interleukin 18 receptor accessory protein
1449399_a_at	Il1b	Mm.222830	7.6	2.E-02	2 F	interleukin 1 beta
1448950_at	Il1r1	Mm.896	4.1	7.E-05	1 B	interleukin 1 receptor, type I
1422317_a_at	Il1rl1	Mm.289824	7.9	2.E-02	1 B	interleukin 1 receptor-like 1
1451798_at	Il1rn	Mm.882	11.7	3.E-04	2 A3	interleukin 1 receptor antagonist
1421034_a_at	Il4ra	Mm.233802	2.9	8.E-04	7 F3	interleukin 4 receptor, alpha
1422053_at	Inhba	Mm.8042	9.3	4.E-03	13 A1	inhibin beta-A
1450501_at	Itga2	Mm.5007	4.1	2.E-03	13 D2.2	integrin alpha 2
1451336_at	Lgals4	Mm.210336	3.5	9.E-04	7 A3	lectin, galactose binding, soluble 4
1416304_at	Litaf	Mm.294753	4.4	5.E-05	16 B1-B3	LPS-induced TN factor
1422352_at	Mcpt1	Mm.201549	11.4	2.E-03	14 C3	mast cell protease 1
1422990_at	Met	Mm.86844	2.9	1.E-03	6 4.0 cM	met proto-oncogene
1417256_at	Mmp13	Mm.5022	14.3	8.E-03	9 A1-A2	matrix metallopeptidase 13
1418945_at	Mmp3	Mm.4993	6.7	7.E-03	9 A1	matrix metallopeptidase 3
1419127_at	Npy	In multiple Genes	3.1	1.E-02		
1419123_a_at	Pdgfc	Mm.331089	3.2	2.E-03	3 E3	platelet-derived growth factor, C polypeptide
1450060_at	Pigr	Mm.276414	6.8	2.E-05	1 E3	polymeric immunoglobulin receptor
1415806_at	Plat	Mm.154660	3.0	1.E-02	8 A2	plasminogen activator, tissue
1452521_a_at	Plaur	Mm.1359	4.8	3.E-03	7 A3	plasminogen activator, urokinase receptor
1457088_at	Pldn	Mm.268921	4.2	2.E-03	2 E5	pallidin
1429527_a_at	Plscr1	Mm.421956	3.4	4.E-04	9 E3.3	phospholipid scramblase 1
1416957_at	Pou2af1	Mm.897	5.8	7.E-04	9 A5.3	POU domain, class 2, associating factor 1
1421073_a_at	Ptger4	Mm.18509	9.0	9.E-06	15 A1	prostaglandin E receptor 4 (subtype EP4)
1417262_at	Ptgs2	Mm.292547	7.0	4.E-02	1 H1	prostaglandin-endoperoxide synthase 2
1420710_at	Rel	Mm.4869	3.0	2.E-02	11 A3.2	reticuloendotheliosis oncogene
1426604_at	Rnasel	Mm.259254	4.2	5.E-04	1 G2	ribonuclease L (2', 5'-oligoisoadenylate synthetase-dependent)
1419394_s_at	S100a8	Mm.21567	6.3	4.E-02	3 F1-F2	S100 calcium binding protein A8 (calgranulin A)
1419480_at	Sell	Mm.1461	3.3	3.E-02	1 H2.2	selectin, lymphocyte
1420558_at	Selp	Mm.3337	3.9	2.E-02	1 H2.2	selectin, platelet
1420378_at	SftpD	Mm.1321	9.5	5.E-05	14 B	surfactant associated protein D
1455899_x_at	Socs3	Mm.3468	5.0	4.E-03	11 E2	suppressor of cytokine signaling 3

1460302_at	Thbs1	Mm.4159	3.5	4.E-02	2 F1-F3	thrombospondin 1
1418685_at	Tirap	Mm.23987	3.7	2.E-05	9 A5.3	toll-interleukin 1 receptor (TIR) domain-containing adaptor protein
1449049_at	Tlr1	Mm.273024	3.4	6.E-03	5 C3.1	toll-like receptor 1
1419132_at	Tlr2	Mm.87596	3.0	1.E-03	3 E3	toll-like receptor 2
1442827_at	Tlr4	Mm.38049	2.8	2.E-03	4 C1	toll-like receptor 4
1418571_at	Tnfrsf12a	Mm.28518	3.6	9.E-04	17 A3.3	tumor necrosis factor receptor superfamily, member 12a
1419083_at	Tnfsf11	Mm.249221	2.9	3.E-02	14 D3	tumor necrosis factor (ligand) superfamily, member 11
1447845_s_at	Vnn1	Mm.27154	21.7	3.E-05	10 A1-B2	vanin 1
1458070_at	Vtcn1	Mm.137467	5.8	1.E-05	3 F2.2	V-set domain containing T cell activation inhibitor 1
1455098_a_at	Vtn	Mm.3667	0.1	5.E-05	11 B5	vitronectin

Supplemental Table 2.**Mouse primer sequences used in quantitative real-time RT-PCR**

Gene	RefSeq No.	Forward primer	Reverse primer	Product Size (bp)
Tff1	NM_009362.2	CCCGGGAGAGGATAAATTGT	GCCAGTTCTCTCAGGATGGA	173
Tnfa	NM_013693.2	CCACCACGCTCTCTGTCTA	AGGGTCTGGGCCATAGAACT	100
Il1β	NM_008361.3	CTTGAAAGAAGAGCCCATCC	CATCTGGAGCCTGTAGTGC	101
Il1α	NM_010554.4	TCAAGATGGCCAAGTTCCCT	TGAGCCATAGCTTCATCAT	131
Cxcl1	NM_008176.3	GCTGGGATTCACCTCAAGAA	TCTCCGTTACTTGGGACAC	180
Cxcl2	NM_009140.2	AGTGAACTGCGCTGTCAATG	TTCAAGGTCAAGGCAAACCT	153
Cxcl5	NM_009141.2	GCCCTACGGTGGAAAGTCATA	GTGCATTCCGCTTAGCTTC	132
Il4α	NM_001008700.3	TTTTGAAGTTGCTGGAGAGG	CGTGGAAAGTGGATGTAGT	100
Vtn1	NM_178594.3	CCTCTCCATGGCTTCCTG	GAAATGCCAAAGCCAATGAT	102
Apoa1	NM_009692.3	GCCAACAGCTAACCTGAAT	CAGAAGTCCGAGTCAATGG	100

Human primer sequences used in quantitative real-time RT-PCR

Gene	RefSeq No.	Forward primer	Reverse primer	Product Size (bp)
TFF1	NM_003225.2	GGTCCTGGTGTCCATGCTG	ACAGCAGCCCTTATTGAC	136
CXCL5	NM_002994.3	GATCCAGAAGCCCCCTTTCT	GAAACTTTCCATGCGTGCT	101
IL-4Rα	NM_000418.2	GGCGCGCAGATAATTAAAGA	GCTGGTCTCGAACTCCTGAT	139
TIRAP	NM_148910.2	CAGCCCTCATCGCAACTG	TTCTAGTGACACTTCTCCTGTGAAA	101
BIRC3	NM_001165.3	TTAACTGGCCCTAGTGTCT	CACCATCACAGCAAAGCAT	105
SMAC	NM_019887.4	TCATAGGAGCCAGAGCTGAGA	TTCTGCTGCCATCTGTGAAA	101

Supplemental Table 3. Calculation of the IHC composite expression score (CES)

		Frequency			
		1	2	3	4
Intensity	0	0	0	0	0
	1	1	2	3	4
	2	5	6	7	8
	3	9	10	11	12

To obtain an IHC continuos score that takes into account the IHC signal intensity and the frequency of positive cells, we generated a composite expression score (CES) with full range from 0 to 12. The CES is calculated using the formula; CES = 4(intensity-1)+frequency.